Chin. Geogra. Sci. 2021 Vol. 31 No. 4 pp. 684−695
https://doi.org/10.1007/s11769-021-1217-5

Springer Science Press
www.springerlink.com/content/1002-0063

Vegetation Index Reconstruction and Linkage with Drought for the Source Region of the Yangtze River Based on Tree-ring Data

LI Jinjian[1], WANG Shu[1, 2], QIN Ningsheng[2], LIU Xisheng[3], JIN Liya[1]

(1. *School of Atmospheric Sciences*, *Plateau Atmosphere and Environment Key Laboratory of Sichuan Province*, *Chengdu University of Information Technology*, *Chengdu* 610225, *China*; 2. *Institute of Plateau Meteorology*, *China Meteorological Administration*, *Chengdu/Heavy Rain and Drought-Flood Disasters in Plateau and Basin*, *Key Laboratory of Sichuan Province*, *Chengdu* 610072, *China*; 3. *Hydrology and Water Resources Bureau of Qinghai Province*, *Xining* 810000, *China*)

Abstract: Variations in vegetation are closely related to climate change, but understanding of their characteristics and causes remains limited. As a typical semi-humid and semi-arid cold plateau region, it is important to understand the knowledge of long term Normalized Difference Vegetation Index (NDVI) variations and find the potential causes in the source region of the Yangtze River. Based on four tree-ring width chronologies, the regional mean NDVI for July and August spanning the period 1665–2013 was reconstructed using a regression model, and it explained 43.9% of the total variance during the period 1981–2013. In decadal, the reconstructed NDVI showed eight growth stages (1754–1764, 1766–1783, 1794–1811, 1828–1838, 1843–1855, 1862–1873, 1897–1909, and 1932–1945) and four degradation stages (1679–1698, 1726–1753, 1910–1923, and 1988–2000). And based on wavelet analysis, significant cycles of 2–3 yr and 3–8 yr were identified. In additional, there was a significant positive correlation between the NDVI and the Palmer Drought Severity Index (PDSI) during the past 349 yr, and they were mainly in phase. However, according to the results of correlation analysis between different grades of drought/wet and NDVI, there was significant asymmetry in extreme drought years and extreme wet years. In extreme drought years, NDVI was positively correlated with PDSI, and in extreme wet years they were negatively correlated.

Keywords: Normalized Difference Vegetation Index (NDVI); reconstruction; dendrochronology; tree ring; Source Region of the Yangtze River

Citation: LI Jinjian, WANG Shu, QIN Ningsheng, LIU Xisheng, JIN Liya, 2021. Vegetation Index Reconstruction and Linkage with Drought for the Source Region of the Yangtze River Based on Tree-ring Data. *Chinese Geographical Science*, 31(4): 684−695. https://doi.org/10.1007/s11769-021-1217-5

1 Introduction

As the main biomass of terrestrial ecosystems, vegetation plays a very important role in the energy conversion and material circulation of the Earth. Vegetation not only responds to climate change but also has feedback effects on it and is an indicator of global change (Piao et al., 2006; Jong et al., 2011). In recent decades, remote sensing data have been extensively used to study vegetation changes, with the development of remote sensing technologies (Tucker et al., 1986; Zhou et al., 2001; Hmimina et al., 2013). The Normalized Difference Vegetation Index (NDVI), determined by the red/near-infrared reflectance of remote sensing images,

Received date: 2020-12-04; accepted date: 2021-04-08

Foundation item: Under the auspices of the Second Tibetan Plateau Scientific Expedition and Research (STEP) Program (No. 2019QZKK0103), National Natural Science Foundation of China (No. 41772173, 41405077), the Thousand Talents Program for High-end Innovation of Qinghai Province, the Applied Basic Research Project of Qinghai Province (No. 2019-zj-7045)

Corresponding author: LI Jinjian. E-mail: ljj@cuit.edu.cn

is a commonly used indicator of the growth status of surface vegetation, which can reflect the coverage, growth conditions, biomass, and photosynthesis of vegetation in a relatively accurate manner (Sellers et al., 1995; Tucker et al., 2001; Ju and Masek, 2016). In recent years, many scholars have conducted extensive studies on the variation characteristics and influencing factors of the NDVI around the world (Hlásny et al., 2015; Liu and Menzel, 2016; Mariano et al., 2018; Zhao et al., 2018; Butterfield et al., 2020). However, because the observation time of the NDVI data is relatively short (since the 1980s), our understanding of the long-term characteristics and influencing factors of vegetation growth and change remains limited.

As a climate proxy, tree-ring data has the characteristics of high accuracy, high resolution, strong continuity, and applicability over a wide geographical range (Cook et al., 2010; Büntgen et al., 2013; PAGES 2k Consortium, 2013; Ljungqvist et al., 2020). It is widely applied in studies of historical climate change, including for the reconstruction of temperature (Anchukaitis et al., 2013; Wilson et al., 2016; Chen et al., 2019a), precipitation (Fritts et al., 1971; Shao et al., 2010; Yang et al., 2014), runoff (Li et al., 2018; Chen et al., 2019b; 2019c), and drought (Cook et al., 2010; Gaire et al., 2019). Recently, researchers found that there was a general positive relationship between annual growth rings and NDVI (Vicente-Serrano et al., 2016; Brehaut and Danby, 2018), and progress has been made in the reconstruction of NDVI data from tree rings. Malmström et al. (1997) first pointed out that NDVI-based Net Primary Productivity (NPP) was significantly correlated with tree-ring width indices collected from Alaska. D'Arrigo et al. (2010) subsequently found a significant correlation between the NDVI and the maximum latewood density of tree rings in coniferous forests in the northern United States. Shishov et al. (2002) focused on the spatial correlation between the tree-ring index and NDVI in Siberia. Furthermore, Leavitt et al. (2008) found a significant positive correlation between the NDVI and $\delta^{13}C$ in tree rings in the southwestern United States. There is evidence that different types of tree-ring measurement can reflect changes in NDVI (Kaufmann et al., 2004; Wang et al., 2004; He and Shao, 2006; Lopatin et al., 2006; Liang et al., 2009; Berner et al., 2011; Wang et al., 2017; Seftigen et al., 2018; Zhang et al., 2018).

The Yangtze River is one of the most important rivers in China. Its source region is located on the southeastern part of the Tibetan Plateau, which is a very important ecological barrier, and a region with sensitive and fragile ecological environments (Yao et al., 2004). Studies have obtained significant results regarding vegetation changes in the Source Region of the Yangtze River (SRYR) and surrounding regions (Zhang et al., 2010; Yang et al., 2011; Bai et al., 2012; Wang et al., 2016; Xia et al., 2019). However, there are no reports on long-term NDVI changes and their causes in the SRYR. Meanwhile, tree rings in this region have been widely used to reconstruct climate and runoff (Qin et al., 2003; Liang et al., 2008; Li et al., 2018; Xiao et al., 2018). In order to understanding the knowledge of NDVI variations of SRYR and finding the potential causes, tree-ring width indices obtained from four tree-ring sampling points in the SRYR and its vicinity were used to explore their relationship with the NDVI, and NDVI variation sequences for July and August spanning the past 349 years were reconstructed to further analyze the variation in vegetation growth, and its correlations with drought and wet years, to predict ecological changes in the SRYR. This study provides a reference for predicting changes in the ecological environment of the SRYR.

2 Data and Methods

2.1 Study area

The source region of the Yangtze River (Fig. 1) in the southwestern Qinghai Province is approximately 738 km from the east to west, and 406 km from the south to north, with an area of approximately 26.2×10^4 km^2 (Qian et al., 2006). The landform is dominated by high plains and hills, with an average elevation of more than 4000 m above sea level (a.s.l.). The monthly average temperature is above 0℃ only from June to September, with the lowest temperature in January (–16.5℃) and the highest temperature in July (6.0℃). The total monthly precipitation ranges from 2 mm (December) to 94 mm (July). Precipitation from May to September (months with relatively high temperatures) accounts for 88.7% of the annual precipitation, and the concurrent warm and wet climatic conditions are favorable for the growth and development of vegetation. The ecosystems in the source region of the Yangtze River principally include alpine steppe, alpine meadow, alpine marsh and wetland, localized and sparsely distributed alpine shrubs

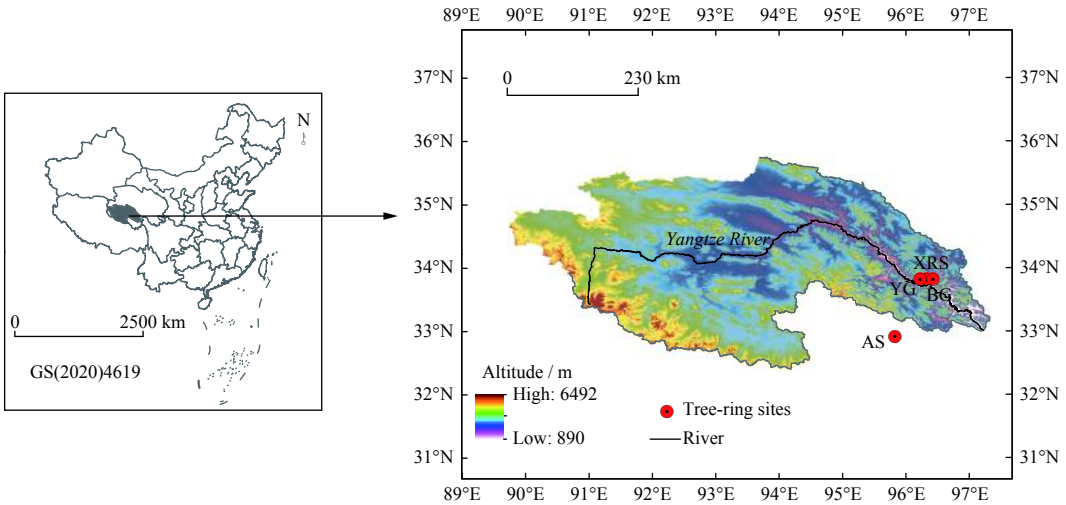

Fig. 1 Location of the tree-ring sample sites at the source region of the Yangtze River. AG, XRS, YG, BG represent the tree-ring sites' ID

in some river valleys, and cushion plants and sparse vegetation on the rock slopes of the high mountains. The NDVI exhibits unimodal pattern, changes only slightly from January to March, and in November and December; therefore, almost no vegetation grows during these periods. It begins to increase in April, when the vegetation enters the rapid growth season, and peaks from July to August (0.37–0.38), when vegetation growth is most active. In September, the NDVI starts to decrease as the vegetation withers. It is evident that the vegetation growth in SRYR is concentrated from May to September, and this period is the main vegetation growth season in this region.

2.2 Tree-ring data and chronology development

We sampled tree-rings at four sites in SRYR in September 2013 (Fig. 1 and Table 1). All the trees were living in remote areas that are rarely influenced by human activities. We used growth cores with a diameter of 5.15 mm and obtained two or three cores from each tree. A total of 203 cores from four sites were used in this study. The COFECHA program (Holmes, 1983) was used after the collected samples were processed by drying, pasting, polishing, and measuring. Cross-dating and verification of the results were performed to ensure accurate dating results. The data were detrended by a negative exponential curve using ARSTAN (Cook, 1985; http://www.ldeo.columbia.edu/tree-ring-laboratory/resources/software). The autoregressive model was then used to eliminate low-frequency variation caused by competition among trees within the forest. Eventually, we obtained three types of chronologies: Standard (STD) chronologies, Residual (RES) chronologies, and ARSTAN (ARS) chronologies. The RES chronologies remove the continuous influence of the special early physiological conditions on the following growth years, and therefore retain more high-frequency signals (Fritts, 1976). Meanwhile, NDVI is sensitive to climate conditions (Hlásny et al., 2015; Mariano et al., 2018; Butterfield et al., 2020), which leads to significant high-frequency variation. Therefore, the RES chronologies were used for reconstruction in this study.

The Mean Sensitivity (MS) and Signal-to-Noise Ratios (SNR) were employed to test whether the chronologies could reveal regional climate and environmental changes (Wang et al., 2016), the higher values suggest

Table 1 Information of the four tree-ring sampling sites in the source region of the Yangtze River

ID	Latitude and Longitude	Altitude / m	Mean sensitivity (MS)	Period with Subsample Signal Strength (SSS) > 0.85 (minimum number of trees)	Signal to Noise Ratio (SNR)	Expressed Population Signal (EPS)
AS	32.9°N, 95.8°E	4042	0.33	1665–2013 (11)	11.98	0.94
XRS	33.8°N, 96.3°E	3979	0.31	1617–2013 (9)	18.89	0.95
YG	33.8°N, 96.2°E	4405	0.31	1568–2013 (13)	13.11	0.93
BG	33.8°N, 96.4°E	4083	0.29	1553–2013 (8)	7.19	0.88

the more climatic signals in tree-ring width. In general, MS > 0.1 and SNR > 5, which suggest the chronology could be used to reconstruct. Meanwhile, the Subsample Signal Strength (SSS) was used to evaluate the reliable starting year, an SSS > 0.85 was used to ensure a reliable chronology length (Liu et al., 2010; Bao et al., 2012). According to Table 1, the MS values of the four chronologies were 0.33, 0.31, 0.31, and 0.29, and the SNR values were 11.98, 18.89, 13.11, and 7.19, suggesting that the radial growth was sensitive to climate and environmental changes. And the reliable period of the four chronologies were 1665–2013, 1617–2013, 1568–2013 and 1553–2013, respectively. As shown in Fig. 2, although the longest distance between the sample sites is nearly 150 km, their variation characteristics are still highly consistent. The correlation coefficients between the chronologies in the common period (1665–2013, n = 349) were 0.395 (AS and BG, $P < 0.0001$), 0.437 (AS and YG, $P < 0.0001$), 0.518 (AS and XRS, $P < 0.0001$), 0.593 (BG and YG, $P < 0.0001$), 0.674 (BG and XRS, $P < 0.0001$), and 0.682 (YG and XRS, $P < 0.0001$).

2.3 Meteorological and NDVI data

Meteorological data, including the mean maximum temperature, mean minimum temperature, mean temperature, precipitation, were provided by China Meteorological Administration, which is a monthly gridded dataset with a spatial resolution of 0.25° × 0.25°. The dataset is based on the observed data from over 2400 weather stations in China. The method of 'anomaly approach', which considering the change of climate factors with altitude, was applied in the dataset production. The details could be found in the reference Xu et al. (2009) and Wu and Gao (2013). The dataset covers the period 1961 to 2018.

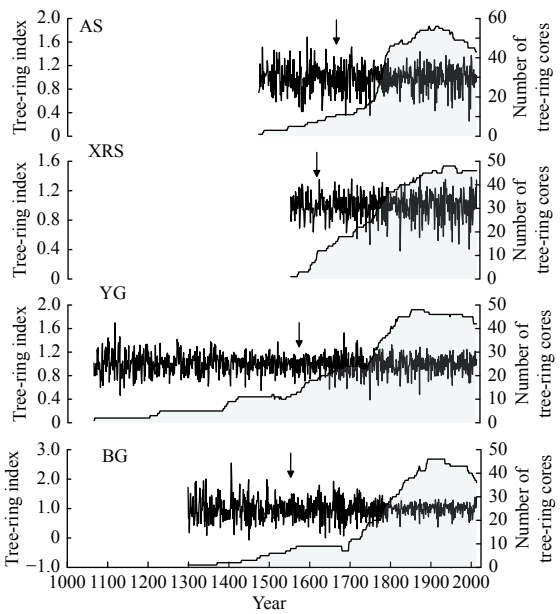

Fig. 2 Tree-ring width Residual (RES) chronologies of the source region of the Yangtze River, and number of cores. The year with Subsample Signal Strength (SSS) > 0.85 is marked by an arrow. AG, XRS, YG, BG represent the tree-ring sites' ID

The Palmer Drought Severity Index (PDSI) data were from the Monsoon Asia Drought Atlas (MADA), which was reconstructed by Cook et al. (2010) using tree-ring data. The dataset covers the period 1300 to 2005, and has a total of 534 grid points and a spatial resolution of 2.5° × 2.5°.

The NDVI dataset provided by Global Inventory Modeling and Mapping Studies (GIMMS) is currently one of the most commonly used vegetation indices. This dataset eliminates the influence of temporal changes on volcanic eruptions, solar elevation angle, and sensor sensitivity (Fensholt et al., 2009), and can effectively represent regional changes in vegetation growth. GIMMS NDVI dataset 3 g.v1 (https://ecocast.arc.nasa.gov/data/pub/gimms/3g.v1/) is a 15 d synthetic dataset from the National Aeronautics and Space Administration's (NASA's) Goddard Space Flight Center, with a spatial resolution of 1/12°, which is about 8 km. It is the longest NDVI dataset, spanning from 1981 to 2015. Monthly NDVI data were obtained using the maximum value composite (MVC) method (Holben, 1986). To exclude the effect of non-vegetation factors, pixels with a multiyear average NDVI smaller than 0.1 were excluded. The NDVI variation dataset of the SRYR can be obtained through preprocessing, such as format conversion, projection transformation, subset extraction, and cropping.

2.4 Methods

The relationships between tree-ring width, climate and then NDVI were analyzed using the Pearson correlations in the SPSS, and then a multivarate linear regression was employed to reconstruct the NDVI. The leave-one-out method (Michaelsen, 1987) was used to test the model's stability and reliability. The testing statistics mainly include Correlation Coefficient (r), Reduced Error (RE), Average Value of the Product (t), and the sign

test. To analyze the characteristics of NDVI changes, we also used some mathematical statistical diagnosis methods including wavelet analysis (Torrence, 1998) and cross-wavelet analysis (Grinsted et al., 2004).

3 Results

3.1 Relationship between tree-ring width, climate, and NDVI

According to Fig. 3, the relationship between the tree-ring width chronology and climatic factors exhibits good consistency at the four sampling points, and the correlation between the tree-ring and precipitation was most significantly positive in May ($r = 0.580$; $P < 0.05$). In terms of temperature, it exhibited significant negative correlations with the mean maximum temperature in May (the highest correlation coefficient was –0.543, $P < 0.05$), meanwhile, the chronology of AS and YG was significant negative correlated with the mean temperature in May as well. And, chronologies had a significant positive correlation with both the mean minimum temperature (the highest correlation coefficient was 0.435, $P < 0.05$) and mean temperature (the highest correlation coefficient was 0.436; $P < 0.05$) in July (except the tree-ring of AS).

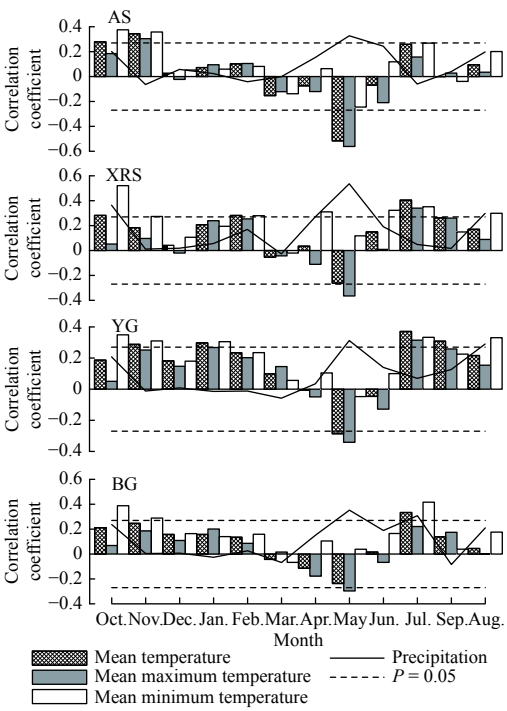

Fig. 3 Correlation analysis between the four tree-ring chronologies and climatic factors from October of the previous year to September of the current year during 1962–2013 in the source region of the Yangtze River. AG, XRS, YG, BG represent the tree-ring sites' ID

Rather than a single climatic factor, the NDVI is jointly affected by various factors, such as precipitation, temperature, and evaporation (Peng et al., 2010; Sun et al., 2013; Wang et al., 2015). Table 2 shows that there were significant correlations ($P < 0.05$) between NDVI and climatic factors (mainly include the monthly average maximum temperature in March to July and September, the monthly average minimum temperature in June and September, the monthly average temperature in March, May to July and September, monthly precipitation in May) in the SRYR. Thus, it exhibited a better correlation with tree-ring, especially during the growth season. Table 3 shows the correlation between the tree-ring and NDVI for each month from 1982 to 2013. The tree-ring was significantly positively correlated with the NDVI of July and August at all four sampling sites with the highest correlation coefficient 0.612. The correlations reached significance at a level of 0.01, indicating that the tree-ring mirrored changes in the NDVI. Therefore, it is feasible to restore the NDVI data using the tree-ring chronology.

3.2 NDVI reconstruction

Based on the above results, because of the significant correlation between tree-ring width and the NDVI of July to August, the RES chronology established from the AS, XRS, YG, and BG tree-ring sampling sites over the period 1982–2013 was selected as the independent variable, while the average NDVI from July to August in SRYR was used as the dependent variable, to establish the following multiple regression equation:

$$P_{NDVI} = 0.326 + 0.011 \times C_{AS} + 0.027 \times C_{BG} + 0.013 \times C_{YG} + 0.006 \times C_{XRS} \quad (1)$$

where P_{NDVI} represents the regional average of the NDVI from July to August in SRYR, C_{AS}, C_{BG}, C_{YG} and C_{XRS} represents RES chronology from tree-ring sites AS, BG, YG, and XRS, respectively. The explained variance (R^2) in the reconstruction equation was 43.9%, and the adjusted explained variance was 35.9%. The correlation coefficient between the reconstructed sequence and the original measured sequence was 0.663 ($n = 33$, $P < 0.01$).

To verify the stability and reliability of the reconstruction equation, it was validated using the leave-one-

Table 2 Correlation between monthly average or growth season average normalized difference vegetation index and climate factors during 1982–2015 in the source region of the Yangtze River

Climate factor	Mar.	Apr.	May	Jun.	Jul.	Aug.	Sep.	Growth season (May to Sep.)
Average maximum temperature	0.509**	0.379*	0.385*	0.425*	0.473**	0.180	0.438*	0.355*
Average minimum temperature	0.210	–0.054	0.161	0.486**	0.322	0.102	0.389*	0.449*
Average temperature	0.422*	0.269	0.384*	0.484**	0.482**	0.171	0.451**	0.425*
Precipitation	–0.336	–0.207	–0.363*	0.050	–0.173	0.084	–0.098	0.125

Notes: *, ** suggested the significance at a level of 0.05 and 0.01, respectively

Table 3 The relationship between the four tree-ring chronologies and monthly normalized difference vegetation index during 1982–2013 in the source region of the Yangtze River

ID	Jan.	Feb.	Mar.	Apr.	May	Jun.	Jul.	Aug.	Sep.	Oct.	Nov.	Dec.	Jul.–Aug.
AS	–0.110	–0.135	–0.028	–0.114	–0.399*	0.292	0.490**	0.510**	0.125	0.082	–0.010	0.026	0.548**
XRS	–0.035	–0.029	–0.030	–0.149	–0.241	0.445**	0.472**	0.549**	0.212	0.244	–0.028	0.072	0.568**
YG	–0.074	–0.067	0.013	–0.212	–0.193	0.275	0.462**	0.568**	0.261	0.268	0.058	0.045	0.567**
BG	–0.020	–0.053	–0.099	–0.119	–0.340*	0.287	0.474**	0.612**	0.161	0.018	–0.150	0.027	0.594**

Notes: *, ** suggests significance at a level of 0.05 and 0.01, respectively

out method, and the relevant statistics are listed in Table 4. The statistical characteristics, including the correlation coefficient (r = 0.663), and average value of the product (t = 3.797), reached significance at a level of 0.01. Reduced Error (RE = 0.521) is positive, which indicates that the reconstruction equation is stable and reliable. The first-order sign test reached significance at a level of 0.05, while the sign test failed to reach significance at a level of 0.05, indicating that the reconstruction equation performed better in the reconstruction of high-frequency variations than low-frequency variations.

3.3 Characteristics of NDVI changes

Using the reconstruction equation, the summer (July and August) NDVI of SRYR from 1665 to 2013 were reconstructed (Fig. 4). The five highest value years were 1718 (value: 0.407), 1873 (0.404), 1673 (0.404), 1780 (0.403) and 1773 (0.401), and the five lowest value years were 1824 (value: 0.353), 1872 (0.353), 1684 (0.354), 1995 (0.355) and 1717 (0.356). To reveal the decadal variations in the growth and degradation periods, an 11-yr moving average was calculated. The growth periods (or degradation period) were defined as periods in which the NDVI was consecutively greater (or lower) than the average of the reconstruction (0.382) for at least 10 yr. There were eight growth stages (1754–1764, 1766–1783, 1794–1811, 1828–1838, 1843–1855, 1862–1873, 1897–1909, and 1932–1945) and four degradation stages (1679–1698, 1726–1753, 1910–1923, and 1988–2000) during the past 349 yr. The longest growth periods were 1766–1783 and 1794–1811, with durations of 18 yr. The longest degradation period was 1726–1753, with a duration of 28 yr.

It is evident from the wavelet analysis (Fig. 5) that there were significant cycles in the NDVI variations, with periods of 2–3 yr and 3–8 yr. The 2–3 yr cycle is consistent with the 'Quasi-Biennial Oscillation', which is a common periodicity in meteorological systems (Mukherjee et al., 1985; Zhou et al., 2009; Shi et al., 2014). The 3–8 yr cycle coincides with the oscillation period of the El Niño-Southern Oscillation (ENSO) (Li et al., 2013), and mainly occurred in the late seven-

Table 4 Statistical parameters of the transfer function and cross-validation for the Normalized Difference Vegetation Index (NDVI) reconstruction during 1982–2013 in source region of the Yangtze River

Correlation coefficient	R^2	Reduced error	The average value of the product	Sign test	First-order sign test
0.663**	0.439	0.521	3.797**	19 (20[a], 21[b])	21 (20[a], 22[b])

Notes: ** the significance at a level of 0.01; a, b: Numbers of identical signs required to reach significance at a level of 0.05 and 0.01, respectively

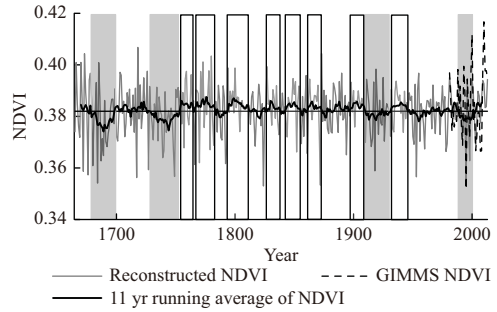

Fig. 4 The changes of reconstructed Normalized Difference Vegetation Index (NDVI) during 1665–2013 and comparison between the observed and reconstructed NDVI during 1982–2013. The period with grey (white) rectangle was degradation (growth) periods

teenth century, late 18 century, and early 19 century. These results are consistent with those of existing studies on the periodic analysis of reconstructed temperature (Liang et al., 2008; Shi et al., 2010), precipitation (Gou et al., 2013; Yang et al., 2014), and runoff (Xiao et al., 2017; Li et al., 2018) in SRYR, indicating that the climatic factors there are affected by large-scale ocean-atmospheric circulations such as the Pacific Decadal Oscillation (PDO) and ENSO, and that atmospheric circulation may affect vegetation growth in SRYR by affecting its climate.

4 Discussion

4.1 Tree-ring growth and climate

The change of NDVI is controlled by many factors, and climate is one of the main factors. Most studies show that temperature and precipitation was the most important factors (Ding et al., 2007; Wang et al., 2015). However, in different regions, the effects of temperature and precipitation are different. The results of previous indicated that the temperature played more important roles (Tang et al., 2006) in three-river source region. In our research, it also exhibited a better correlation between NDVI and temperature. This may be related to the vegetation, climate and landform of the study area (Tang et al., 2006). Our samples were taken from SRYR, an area located in the eastern part of the Tibetan Plateau. During the early growth season, the significant positive correlation between tree radial growth and precipitation, and the significant negative correlation between tree radial growth and temperature, may indicate that an increase in temperature can result in enhanced evaporation and plant transpiration, thereby exacerbating the water stress effect and inhibiting the growth of trees, while an increase in precipitation could be conducive to tree growth. Similar conclusions have been confirmed in previous studies (Qin et al., 2003; Gou et al., 2008; Shi et al., 2010). However, during July, the positive correlation between tree radial growth, precipitation, and temperature, suggests that concurrent rain and heat are conducive to photosynthesis, resulting in wide rings (Liang et al., 2008). There is a high statistical correlation between the tree ring width chronology and NDVI. The radial growth of trees is related to the climatic conditions in the growing season. NDVI reflects the growth status of vegetation and is also related to the climatic and environmental conditions, indicating that there is consistency in the response of the two to the limiting factors.

4.2 Linkage between the NDVI and PDSI

The growth conditions of vegetation are constrained by

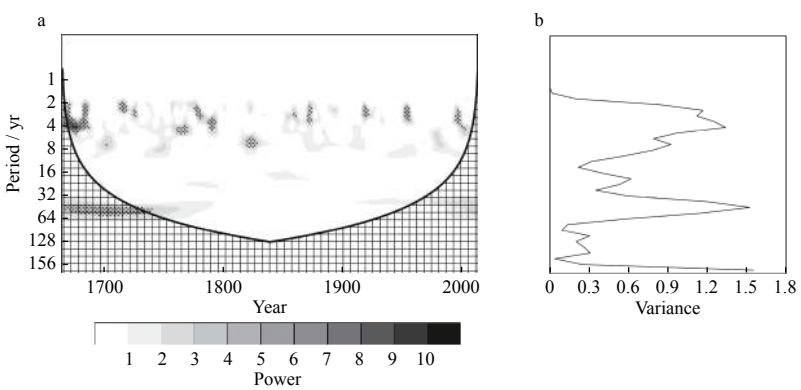

Fig. 5 The wavelet power spectrum (a) and wavelet variance (b) of the wavelet analysis of reconstructed Normalized Difference Vegetation Index (NDVI). The dotted areas suggest significance at a level of 0.05 and the areas with grid line indicate the cone of influence

a variety of factors, among which climate is one of the most important. Among all climatic factors, drought is considered to be of key influence on vegetation. The PDSI was calculated based on precipitation, temperature, soil moisture, *etc*., and is representative of the regional extent of drought and wet conditions (Palmer, 1965; Dai et al., 2004). Increasing evidence suggests that NDVI series could capture the signals of drought events, especially extreme drought events (Wang et al., 2017; Zhang et al., 2018). As shown in Fig. 6, there were significantly positively correlated in SRYR and its vicinity between the reconstructed NDVI and PDSI during the period 1665–2005, with the correlation coefficient between the mean PDSI and the reconstructed NDVI of the SRYR was 0.611, which reached significance at a level of 0.001. The comparison with other hydro-climatic reconstructions suggests low NDVI period often matched drought period. For example, the low NDVI period 1910–1923 was matched the 1910s–1920s drought periods which widely occurred in central and western China (Bao et al., 2012; Yang et al., 2014; Li et al., 2018). To specifically examine the relationship between drought and NDVI, cross-wavelet analysis was used to show the coherence and phase lag between the NDVI and PDSI (Fig. 7). The result indicates significant resonance between the NDVI and PDSI at scales of quasi 4 yr, quasi 8 yr, and quasi 32 yr. The resonance of quasi 4 yr was found in 1650–1700, 1750–1800, 1860–1980, and 1950–1970. The resonance of quasi 8 yr occurred in 1740–1760, 1830–1850, 1940–1960, and 1980–2000. There was a quasi 32 yr resonance in 1900–1950. Furthermore, a nearly horizontal rightward arrow was in resonance of quasi 4 yr and quasi 8 yr, suggesting that the NDVI and PDSI signals were in phase. A right-downward arrow with an approximately 30° phase angle in the quasi 32 yr resonance indicated that the PDSI led the NDVI change by 1/8 cycle, which is approximately 4 yr.

This result indicates that overall, the degree of wet and drought in the SRYR will significantly positively impact the growth of local vegetation, with wetter conditions leading to better vegetation and vice versa. However, an ensuing question is what the impact of different levels of drought and wetness on the NDVI is? To answer this question, the wet and dry years were firstly defined according to the mean and Standard Deviation (SD) of the PDSI series (Table 5). During the

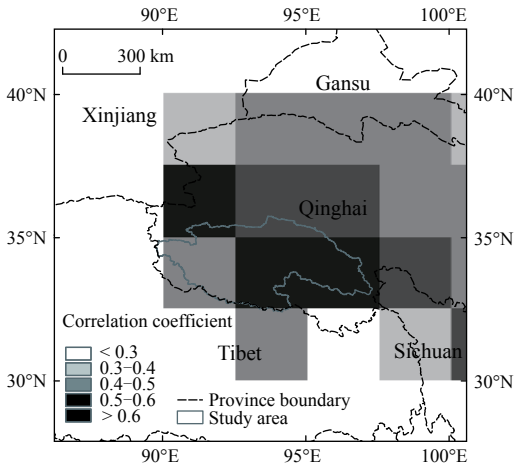

Fig. 6 The correlation coefficient between Normalized difference Vegetation Index (NDVI) and Palmer Drought Severity Index (PDSI) from 1665–2005 around the source region of the Yangtze River

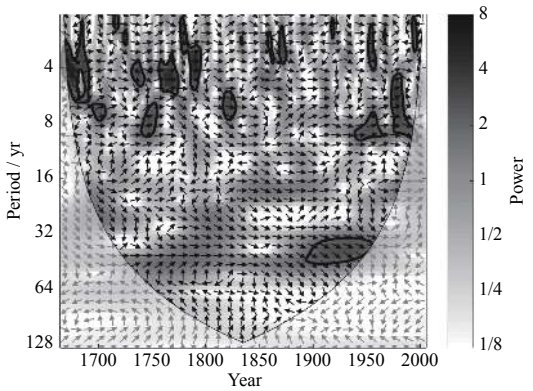

Fig. 7 The wavelet coherence and phase between Normalized Difference Vegetation Index (NDVI) and Palmer Drought Severity Index (PDSI). The vectors indicate the phase difference between NDVI and PDSI; a horizontal arrow pointing from left to right signifies their being in phase. The thick black line is the 95% significance level and the thin black line indicates the cone of influence

Table 5 The standard of wetness and dryness according to the mean and Standard Deviation (SD)

Values	Grade of wet/drought
PDSI<mean–1.5SD	Extreme drought
Mean–1.5SD<PDSI<mean–SD	Drought
Mean–SD<PDSI<mean+SD	Normal
Mean+SD<PDSI<mean+1.5SD	Wet
Mean+1.5SD<PDSI	Extreme wet

Note: Palmer Drought Severity Index (PDSI)

period 1665–2005, the number of normal years was the highest, 252 yr, accounting for 73.9% of the total; the

number of drought (wet) years was 20 yr (27 yr), accounting for 5.9% (7.9%) of the total; the number of extreme drought (extreme wet) years was 25 yr (17 yr), accounting for 7.3% (5.0%) of the total. The frequency of extreme drought years was higher than that of extreme wet years, while the frequency of wet years was higher than that of drought years. Then, the NDVI and PDSI in years corresponding to different drought and wetness grades were extracted for correlation analysis, and the results (Table 6) show that different grades of drought and wet exhibited distinctly different impacts on the NDVI: in normal years, the PDSI and NDVI had significant positive correlations, and the correlation coefficient reached 0.465, indicating that better water conditions resulted in better vegetation, and vice versa. In the dry and wet years, there was still a positive correlation, although it failed to pass the significance test, suggesting that in drought or wet years, the water condition was no longer the key limiting factor. The cause of this phenomenon requires further investigation and discussion. In the extreme drought years, the PDSI and NDVI were positively correlated, with a correlation coefficient of 0.429, and the correlation reached significance at a level of 0.05, indicating that the water condition was one of the most important limiting factors in extreme drought years. However, in extreme wet years, the PDSI and NDVI exhibited significant negative correlations, and the correlation coefficient reached –0.681, reaching significance at a level of 0.01, which was possibly because the study region has a cold plateau climate; the average temperature in summer is less than 10℃, and the temperature difference between sunny days and cloudy days is typically large. Generally, extreme wetness means more precipitation and long-term rainy days, which may lead to lower temperatures and less sunshine, thus limiting vegetation growth. Excessive precipitation can lead to waterlogging, reducing the oxygen content of the soil and thus affecting photosynthesis, causing vegetation to wither (Nakano, 2007; Ashraf and Harris, 2013).

5 Conclusions

The analysis of correlations between the tree-ring width chronology, NDVI, and climatic factors of the SRYR, indicates that the tree-ring width chronology is most significantly correlated with the NDVI of July and August. Thus, we developed a stable and reliable multiple regression equation to reconstruct the summer NDVI in the SRYR over the past 349 yr. During this period, there were eight growth stages and four degradation stages. The growth stages were 1754–1764, 1766–1783, 1794–1811, 1828–1838, 1843–1855, 1862–1873, 1897–1909, and 1932–1945; the degradation stages were 1679–1698, 1726–1753, 1910–1923, and 1988–2000. There were significant cycles of 2–3 yr and 3–8 yr, indicating that vegetation growth might be affected by large-scale ocean-atmospheric circulations, such as PDO and ENSO The reconstructed NDVI and the PDSI of the SRYR and its vicinity were significantly positively correlated, but the correlation showed significant asymmetry in extreme drought years and extreme wet years. In extreme drought years, the PDSI and NDVI were positively correlated, whereas in extreme wet years, the PDSI and NDVI had a significant negative correlation.

This paper provides a long time scale data of local vegetation changes, and reveals that the vegetation growth in SRYR is restricted by the large spatial climate. Also, it was found that there was significant asymmetry in extreme drought years and extreme wet years. This will provide support for future study on the dynamic consistency of vegetation growth. However, this study is still limited because out reconstruction is only based on four sampling sites. Therefore, it is critical to develop a wide tree-ring network in China, even in the whole northern hemisphere. It could help to verify the relative study results and to better understand the impact of climate change on ecological environment.

Table 6 Statistics for graded drought and wet years, and correlations between Palmer Drought Severity Index (PDSI) of drought/wet years and the corresponding Normalized Difference Vegetation Index (NDVI) during 1665–2005 in source region of the Yangtze River

	Extreme drought years	Drought years	Normal years	Wet years	Extreme wet years
Number of years/Percentage	25/7.3%	20/5.9%	252/73.9%	27/7.9%	17/5.0%
Correlation coefficient	0.429*	0.229	0.465**	0.136	–0.681**

Notes: *, ** suggests significance at a level of 0.05 and 0.01, respectively

References

Anchukaitis K J, D'Arrigo R D, Andreu-Hayles L et al., 2013. Tree-ring-reconstructed summer temperatures from northwestern north America during the last nine centuries. *Journal of Climate*, 26(10): 3001–3012. doi: 10.1175/jcli-d-11-00139.1

Ashraf M, Harris, P J C, 2013. Photosynthesis under stressful environments: an overview. *Photosynthetica*, 51: 163–190. doi: 10.1007/s11099-013-0021-6

Bai Shuying, Wang Li, Shi Jianqiao, 2012. Time lag effect of NDVI response to climatic change in Yangtze river basin. *Chinese Journal of Agrometeorology*, 33(4): 579–586. (in Chinese)

Bao G, Liu Y, Liu N, 2012. A tree-ring-based reconstruction of the Yimin River annual runoff in the Hulun Buir region, Inner Mongolia, for the past 135 years. *Chinese Science Bulletin*, 57: 4765–4775. doi: 10.1007/s11434-012-5547-7

Brehaut L, Danby R K, 2018. Inconsistent relationships between annual tree ring-widths and satellite-measured NDVI in a mountainous subarctic environment. *Ecological Indicators*, 91: 698–711. doi: 10.1016/j.ecolind.2018.04.052

Berner L T, Beck P S A, Bunn A G et al., 2011. High-latitude tree growth and satellite vegetation indices: Correlations and trends in Russia and Canada (1982–2008). *Journal Geophysical Research-Biogeosciences*, 116: 321–342. doi: 10.1029/2010JG001475

Büntgen U, Kyncl T, Ginzler C et al., 2013. Filling the eastern european gap in millennium-long temperature reconstructions. *Proceedings of the National Academy of Sciences of the United States of America*, 110(5): 1773–1778. doi: 10.1073/pnas.1211485110

Butterfield Z, Buermann W, Keppel-Aleks G, 2020. Satellite observations reveal seasonal redistribution of northern ecosystem productivity in response to interannual climate variability. *Remote Sensing of Environment*, 242: 111755. doi: 10.1016/j.rse.2020.111755

Cook E R, 1985. *A Time Series Analysis Approach to Tree Ring Standardization*. Tuscon: University of Arizona.

Cook E R, Anchukaitis K J, Buckley B M et al., 2010. Asian monsoon failure and megadrought during the last millennium. *Science*, 328(5977): 486–489. doi: 10.1126/science.1185188

Chen F, Yuan Y J, Yu S L et al., 2019a. A 391-year summer temperature reconstruction of the Tien Shan, reveals far-reaching summer temperature signals over the mid-latitude Eurasian continent. *Journal Geophysical Research: Atmospheres*, 22(124): 11850–11862. doi: 10.1029/2019JD030301

Chen F, Shang H M, Panyushkina I P et al., 2019b. Tree-ring reconstruction of Lhasa River streamflow reveals 472 years of hydrologic change on southern Tibetan Plateau. *Journal of Hydrology*, 572: 169–178. doi: 10.1016/j.jhydrol.2019.02.054

Chen F, Shang H M, Panyushkina I et al., 2019c. 500-year tree-ring reconstruction of Salween River streamflow related to the history of water supply in Southeast Asia. *Climate Dynamics*, 53: 6595–6607. doi: 10.1007/s00382-019-04948-1

Dai A G, Trenberth K E, Qian T T, 2004. A global data set of Palmer Drought Severity Index for 1870−2002: relationship with soil moisture and effects of surface warming. *Journal of Hydrometeorology*, 5: 1117–1130. doi: 10.1175/JHM-386.1

D'Arrigo R D, Malmström C M, Jacoby G C et al., 2010. Correlation between maximum latewood density of annual tree rings and NDVI based estimates of forest productivity. *International Journal of Remote Sensing*, 21(11): 2329–2336. doi: 10.1080/01431160050029611

Ding M J, Zhang Y L, Liu L S et al., 2007. The relationship between NDVI and precipitation on the Tibetan Plateau. *Journal of Geographical Sciences*, 17(3): 259–268. doi: 10.1007/s11442-007-0259-7

Fensholt R, Rasmussen K, Nielsen T T et al., 2009. Evaluation of earth observation based long term vegetation trends Intercomparing NDVI time series trend analysis consistency of Sahel from AVHRR GIMMS, Terra MODIS and SPOT VGT data. *Remote Sensing of Environment*, 113(9): 1886–1898. doi: 10.1016/j.rse.2009.04.004

Fritts H C, Blasing T J, Hayden B P et al., 1971. Multivariate techniques for specifying tree-growth and climate relationships and for reconstructing anomalies in paleoclimate. *Journal of Applied Meteorology and Climatology*, 10(5): 845–864. doi: 10.1175/1520-0450(1971)010<0845:MTFSTG>2.0.CO;2

Fritts H C, 1976. *Tree Rings and Climate*. London: Academic Press, 30–265.

Gaire N P, Dhakal Y R, Shah S K et al., 2019. Drought (scPDSI) reconstruction of trans-himalayan region of central himalaya using pinus wallichiana tree-rings. *Palaeogeography Palaeoclimatology Palaeoecology*, 514: 251–264. doi: 10.1016/j.palaeo.2018.10.026

Grinsted A, Moore J C, Jevrejeva S, 2004. Application of the cross wavelet transform and wavelet coherence to geophysical time series. *Nonlinear Processes in Geophysics*, 11: 561–566. doi: 10.5194/npg-11-561-2004

Gou X H, Peng J F, Chen F H et al., 2008. A dendrochronological analysis of maximum summer half year temperature variations over the past 700 years on the northeastern Tibetan Plateau. *Theoretical and Applied Climatology*, 93(3): 195–206. doi: 10.1007/s00704-007-0336-y

Gou X H, Yang T, Gao L L et al., 2013. A 457-year reconstruction of precipitation in the southeastern Qinghai-Tibet Plateau, China using tree-ring records. *Chinese Science Bulletin*, 58(11): 978–985. doi: 10.1007/s11434-012-5539-7

He J, Shao X M, 2006. Relationships between tree-ring width index and NDVI of grassland in Delingha. *Chinese Science Bulletin*, 51(9): 1083–1090. doi: 10.1007/s11434-006-1106-4

Hlásny T, Barka I, Sitková Z et al., 2015. Modis-based vegetation index has sufficient sensitivity to indicate stand-level intra-seasonal climatic stress in oak and beech forests. *Annals of Forest Science*, 72(1): 109–125. doi: 10.1007/s13595-014-0404-2

Holben B N, 1986. Characteristics of maximum-value composite images from temporal AVHRR data. *International Journal of Remote Sensing*, 7(11): 1417–1434. doi: 10.1080/01431168608948945

Holmes R L, 1983. Computer-assisted quality control in tree-ring dating and measurement. *Tree-Ring Bulletin*, 43: 69–75.

Hmimina G, Dufrêne E, Pontailler J Y et al., 2013. Evaluation of

the potential of MODIS satellite data to predict vegetation phenology in different biomes: an investigation using ground-based NDVI measurements. *Remote Sensing of Environment*, 132(6): 145–158. doi: 10.1016/j.rse.2013.01.010

Jong R D, Bruin S D, Wit A D et al., 2011. Analysis of monotonic greening and browning trends from global NDVI time-series. *Remote Sensing of Environment*, 115(2): 692–702. doi: 10.1016/j.rse.2010.10.011

Ju J C, Masek J G, 2016. The vegetation greenness trend in Canada and US Alaska from 1984−2012 Landsat data. *Remote Sensing of Environment*, 176: 1–16. doi: 10.1016/j.rse.2016.01.001

Kaufmann R K, D'Arrigo R D, Laskowski C et al., 2004. The effect of growing season and summer greenness on northern forests. *Geophysical Research Letters*, 31(9): L09205. doi: 10.1029/2004GL019608

Leavitt S W, Chase T N, Rajagopalan B et al., 2008. Southwestern US tree-ring carbon isotope indices as a possible proxy for reconstruction of greenness of vegetation. *Geophysical Research Letters*, 35(12): 150–152. doi: 10.1029/2008GL033894

Liang E Y, Eckstein D, Liu H Y, 2009. Assessing the recent grassland greening trend in a long-term context based on tree-ring analysis: a case study in North China. *Ecological Indicators*, 9(6): 1280–1283. doi: 10.1016/j.ecolind.2009.02.007

Liang E Y, Shao X M, Qin N S, 2008. Tree-ring based summer temperature reconstruction for the the source region of the Yangtze River on the Tibetan Plateau. *Global and Planetary Change*, 61(3-4): 313–320. doi: 10.1016/j.gloplacha.2007.10.008

Liu Z Y, Menzel L, 2016. Identifying long-term variations in vegetation and climatic variables and their scale-dependent relationships: a case study in southwest germany. *Global and Planetary Change*, 147: 54–66. doi: 10.1016/j.gloplacha.2016.10.019

Liu Y, Sun J Y, Song H M et al., 2010. Tree-ring hydrologic reconstructions for the Heihe River watershed, western China since AD 1430. *Water Research*, 44(9): 2781–2792. doi: 10.1016/j.watres.2010.02.013

Li J J, Shao X M, Qin N S et al., 2018. Runoff variations at the source of the Yangtze River over the past 639 years based on tree-ring data. *Climate Research*, 75(2): 131–142. doi: 10.3354/cr01510

Li J B, Xie S P, Cook E R et al., 2013. El Niño modulations over the past seven centuries. *Nature Climate Change*, 3(9): 822–826. doi: 10.1038/nclimate1936

Lopatin E, Kolström T, Spiecker H, 2006. Determination of forest growth trends in Komi Republic (northwestern Russia): combination of tree-ring analysis and remote sensing data. *Boreal Environment Research*, 11(5): 341–353.

Ljungqvist F C, Piermattei A, Seim A et al., 2020. Ranking of tree-ring based hydroclimate reconstructions of the past millennium. *Quaternary Science Reviews*, 230: 106074. doi: 10.1016/j.quascirev.2019.106074

Malmström C M, Thompson M V, Juday G P et al., 1997. Interannual variation in global-scale net primary production: testing model estimates. *Global Biogeochemical Cycles*, 11(3): 367–392. doi: 10.1029/97GB01419

Mariano D A, Dos Santos C A C, Wardlow B D et al., 2018. Use of remote sensing indicators to assess effects of drought and human-induced land degradation on ecosystem health in northeastern brazil. *Remote Sensing of Environment*, 213: 129–143. doi: 10.1016/j.rse.2018.04.048

Michaelsen J, 1987. Cross-validation in statistical climate forecast models. *Journal of Applied Meteorology*, 26(11): 1589–1600. doi: 10.1175/1520-0450(1987)026<1589:CVISCF>2.0.CO;2

Mukherjee B K, Indira K, Reddy R S et al., 1985. Quasi-biennial oscillation in stratospheric zonal wind and Indian Summer monsoon. *Monthly Weather Review*, 113(8): 1421–1424. doi: 10.1175/1520-0493(1985)113<1421:QBOISZ>2.0.CO;2

Nakano Y, 2007. Response of tomato root systems to environmental stress under soilless culture. *Japan Agricultural Research Quarterly*, 41(1): 7–15. doi: 10.6090/jarq.41.7

PAGES 2k Consortium, 2013. Continental-scale temperature variability during the past two millennia. *Nature Geoscience*, 6(6): 339–346. doi: 10.1038/ngeo1797

Palmer W C, 1965. *Meteorological Drought*. Washington DC: US Department of Commerce, Weather Bureau.

Peng J F, Gou X H, Chen F H et al., 2010. Climate-growth relationships of *Qilian juniper sabina przewalskii* in the Anyemaqen Mountains, Tibet. *Climate Research*, 41(1): 31–40. doi: 10.3354/cr00834

Piao S L, Friedlingstein P, Ciais P et al., 2006. Effect of climate and CO_2 changes on the greening of the Northern Hemisphere over the past two decades. *Geophysical Research Letters*, 33(23): 265–288. doi: 10.1029/2006GL028205

Qian J, Wang G X, Ding Y J et al., 2006. The land ecological evolutional patterns in the source areas of the Yangtze and Yellow Rivers in the past 15 years, China. *Environmental Monitoring and Assessment*, 116(1-3): 137–156. doi: 10.1007/s10661-006-7232-2

Qin N S, Shao X M, Jin L Y et al., 2003. Climate change over southern Qinghai Plateau in the past 500 years recorded in Sabina tibetica tree rings. *Chinese Science Bulletin*, 48(19): 2068–2072. doi: 10.1360/03wd0088

Sellers P J, Meeson B W, Hall F G et al., 1995. Remote sensing of the land surface for studies of global change: models-algorithms-experiments. *Remote Sensing of Environment*, 51(1): 3–26. doi: 10.1016/0034-4257(94)00061-Q

Seftigen K, Frank D C, Björklund J et al., 2018. The climatic drivers of normalized difference vegetation index and tree-ring-based estimates of forest productivity are spatially coherent but temporally decoupled in northern hemispheric forests. *Global Ecology and Biogeography*, 27(11): 1352–1365. doi: 10.1111/geb.12802

Shao X M, Xu Y, Yin Z Y et al., 2010. Climatic implications of a 3585-year tree-ring width chronology from the northeastern Qinghai-Tibetan Plateau. *Quaternary Science Reviews*, 29(17−18): 2111–2122. doi: 10.1016/j.quascirev.2010.05.005

Shi F, Li J P, Wilson R J S, 2014. A tree-ring reconstruction of the South Asian summer monsoon index over the past millennium. *Scientific Reports*, 4: 6739. doi: 10.1038/srep06739

Shishov V V, Vaganov E A, Hughes M K et al., 2002. Spatial

variations in the annual tree-ring growth in Siberia in the past century. *Doklady Earth Sciences*, 387A(9): 1088–1091.

Shi X H, Qin N S, Zhu H F et al., 2010. May−June mean maximum temperature change during 1360−2005 as reconstructed by tree rings of *Sabina Tibetica* in Zaduo, Qinghai Province. *Chinese Science Bulletin*, 55(26): 3023–3029. doi: 10.1007/s11434-010-3237-x

Sun J, Cheng G W, Li W P et al., 2013. On the Variation of NDVI with the principal climatic elements in the Tibetan Plateau. *Remote Sensing*, 5(4): 1894–1911. doi: 10.3390/rs5041894

Tang Hongyu, Xiao Fengjin, Zhang Qiang et al., 2006. Vegetation change and its response to climate change in three-river source region. *Climate Change Research*, 2(4): 177–180. (in Chinese)

Torrence C, Compo G P, 1998. A practical guide to wavelet analysis. *Bulletin of the American Meteorological Society*, 79(1): 61–78. doi: 10.1175/1520-0477(1998)079<0061:APGTWA>2.0.CO;2

Tucker C J, Fung I Y, Keeling C D et al., 1986. Relationship between atmospheric CO_2 variations and a satellite-derived vegetation index. *Nature*, 319(6050): 195–199. doi: 10.1038/319195a0

Tucker C J, Slayback D A, Pinzon J E et al., 2001. Higher northern latitude normalized difference vegetation index and growing season trends from 1982 to 1999. *International Journal of Biometeorology*, 45(4): 184–190. doi: 10.1007/s00484-001-0109-8

Vicente-Serrano S M, Camarero J J, Olano J M et al., 2016. Diverse relationships between forest growth and the Normalized Difference Vegetation Index at a global scale. *Remote Sensing of Environment*, 187: 14–29. doi: 10.1016/j.rse.2016.10.001

Xiao D M, Huang X M, Qin N S, 2018. Tree-ring based annual precipitation reconstruction for the southern Three-River Headwaters region, China. *Journal of Water and Climate Change*, 9(3): 610–623. doi: 10.2166/wcc.2018.190

Wang J, Rich P M, Price K P et al., 2004. Relations between NDVI and tree productivity in the central Great Plains. *International Journal of Remote Sensing*, 25(16): 3127–3138. doi: 10.1080/0143116032000160499

Wang X Y, Yi S H, Wu Q B et al., 2016. The role of permafrost and soil water in distribution of alpine grassland and its NDVI dynamics on the Qinghai-Tibetan Plateau. *Global and Planetary Change*, 147: 40–53. doi: 10.1016/j.gloplacha.2016.10.014

Wang S H, Sun W, Li S W et al., 2015. Interannual variation of the growing season maximum normalized difference vegetation index, MNDVI, and its relationship with climatic factors on the Tibetan Plateau. *Polish Journal of Ecology*, 63(3): 424–439. doi: 10.3161/15052249PJE2015.63.3.012

Wang H Q, Chen F, Zhang R B et al., 2017. Seasonal dynamics of vegetation of the central loess plateau (China) based on tree rings and their relationship to climatic warming. *Environment, Development and Sustainability*, 19(6): 1–12. doi: 10.1007/s10668-016-9870-z

Wilson R, Anchukaitis K, Briffa K R et al., 2016. Last millennium northern hemisphere summer temperatures from tree rings: Part I: the long term context. *Quaternary Science Reviews*, 134(10): 1–18. doi: 10.1016/j.quascirev.2015.12.005

Wu Jia, Gao Xuejie, 2013. A gridded daily observation dataset over China region and comparison with the other datasets. *Chinese Journal of Geophysics*, 56(4): 1102–1111. (in Chinese)

Xiao D M, Shao X M, Qin N S et al., 2017. Tree-ring-based reconstruction of streamflow for the Zaqu River in the Lancang River source region, China, over the past 419 years. *International Journal of Biometeorology*, 61: 1173–1189. doi: 10.1007/s00484-016-1297-6

Xia J, Yi G H, Zhang T B et al., 2019. Interannual variation in the start of vegetation growing season and its response to climate change in the Qinghai-Tibet Plateau derived from MODIS data during 2001 to 2016. *Journal of Applied Remote Sensing*, 13(4): 048506. doi: 10.1117/1.JRS.13.048506

Xu Y, Gao X J, Shen Y et al., 2009. A daily temperature dataset over China and its application in validating a RCM simulation. *Advances in Atmospheric Sciences*, 26: 763–772. doi: 10.1007/s00376-009-9029-z

Yao T D, Wang Y Q, Liu S Y et al., 2004. Recent glacial retreat in High Asia in China and its impact on water resource in Northwest China. *Science in China Series D Earth Sciences*, 47(12): 1065–1075. doi: 10.1360/03yd0256

Yang B, Qin C, Wang J L et al., 2014. A 3,500-year tree-ring record of annual precipitation on the northeastern Tibetan Plateau. *Proceedings of the National Academy of Sciences of the United States of America*, 111(8): 2903–2908. doi: 10.1073/pnas.1319238111

Yang Z P, Gao J X, Zhou C P et al., 2011. Spatio-temporal changes of NDVI and its relation with climatic variables in the source regions of the Yangtze and Yellow rivers. *Journal of GeographicalSciences*,21(6):979–993.doi:10.1007/s11442-011-0894-x

Zhang L, Chen X L, Cai X B et al., 2010. Spatial-temporal changes of NDVI and their relations with precipitation and temperature in Yangtze River basin from 1981 to 2001. *Geospatial Information Science*, 13(3): 186–190. doi: 10.1007/s11806-010-0339-1

Zhao L, Dai A G, Dong B, 2018. Changes in global vegetation activity and its driving factors during 1982–2013. *Agricultural and Forest Meteorology*, 249: 198–209. doi: 10.1016/j.agrformet.2017.11.013

Zhang T W, Zhang R B, Lu B et al., 2018. *Picea schrenkiana* tree-ring chronologies development and vegetation index reconstruction for the Alatau Mountains, Central Asia. *Geochronometria*, 45(1): 107–118. doi: 10.1515/geochr-2015-0091

Zhou L M, Tucker C J, Kaufmann R K et al., 2001. Variations in northern vegetation activity inferred from satellite data of vegetation index during 1981 to 1999. *Journal of Geophysical Research-Atmospheres*, 106(D17): 20069–20083. doi: 10.1029/2000JD000115

Zhou X J, Zhao P, Liu G, 2009. Asian-Pacific Oscillation index and variation of East Asian summer monsoon over the past millennium. *Chinese Science Bulletin*, 54(20): 3768–3771. doi: 10.1007/s11434-009-0619-z